https://doi.org/10.5194/egusphere-2026-4403
Preprint. Discussion started: 7 August 2026

Analytical strategies for $^{207}Pb/^{235}U$ carbonate geochronology

Dawid Szymanowski[1], Marcel Guillong[1], Pieter Vermeesch[2], Philip J. Hopley[3]

[1]Department of Earth and Planetary Sciences, ETH Zurich, 8092 Zurich, Switzerland
[2]Department of Earth Sciences, University College London, London WC1E 6BT, United Kingdom
[3]School of Natural Sciences, Birkbeck, University of London, London WC1E 7HX, United Kingdom

Correspondence to: Dawid Szymanowski (dawid.szymanowski@eaps.ethz.ch)

Abstract. In carbonate U–Pb geochronology, unknown initial $^{234}U/^{238}U$ disequilibria can be debilitating for the accuracy of $^{206}Pb/^{238}U$ dates. Even if residual $^{234}U/^{238}U$ disequilibrium can be measured precisely enough to perform accurate corrections, beyond ca. 1.5 Ma (depending on the magnitude of initial excess/deficit of ^{234}U) the expansion of uncertainties due to the disequilibrium correction may make carbonate $^{206}Pb/^{238}U$ dates prohibitively imprecise. An alternative approach utilising the $^{207}Pb/^{235}U$ system is arguably more accurate, however the lower abundance of ^{235}U and ^{207}Pb relative to ^{238}U and ^{206}Pb inevitably results in larger analytical data-point uncertainties. Here we explore analytical strategies that maximise the potential of the $^{207}Pb/^{235}U$ system for carbonate geochronology. ID-TIMS and LA-ICPMS are considered the most useful, and complementary, techniques. ID-TIMS offers the ultimate precision and accuracy combined with the ability to filter data for contamination using $^{208}Pb/^{204}Pb$, but it requires mg-sized samples that limit the spatial resolution and the spread of data along the isochron. Optimised LA-ICPMS with large spot sizes may be a quick alternative with better spatial control and enhanced spread of data along the isochron, but ^{208}Pb normalisation imposed by the difficulty of analysing ^{204}Pb may add noise to the results. Overall, precise $^{207}Pb/^{235}U$ carbonate geochronology is feasible and with minor analytical adjustments it can be adopted broadly instead of the $^{206}Pb/^{238}U$ method. Future work on carbonates should obtain additional compositional information that will allow robust identification of domains contaminated with extraneous Pb.

1 Introduction

Carbonate rocks, ubiquitous in low-temperature settings, contain archives of Earth's climate and environment, which makes them exciting targets for geochronology. Even though their U content rarely exceeds several parts per million, it is sufficiently high to conduct $^{230}Th/U$ dating in young (< ca. 600 ka) samples that are out of U-series secular equilibrium (Kaufman and Broecker, 1965). Geochronology of older samples needs to rely on the full U–Pb decay scheme. The default method (Roberts et al., 2020) uses the $^{206}Pb/^{238}U$ system which is more accessible analytically than $^{207}Pb/^{235}U$, a result of the disparity between the decay constants of ^{238}U and ^{235}U and their 138-fold difference in abundance in present-day rocks.

However, the $^{206}Pb/^{238}U$ method faces a significant limitation. ^{234}U, an intermediate daughter in the ^{238}U decay chain, is frequently fractionated from its parent in low-temperature environments (Porcelli and Swarzenski, 2003), which results in

https://doi.org/10.5194/egusphere-2026-4403
Preprint. Discussion started: 7 August 2026

common excesses or deficits of the ultimate daughter ^{206}Pb once the system returns to secular equilibrium. The impact of this effect varies with the initial $^{234}U/^{238}U$ disequilibrium value (activity ratio marked with square brackets, $[^{234}U/^{238}U] = (\lambda_{234}{}^{234}U)/(\lambda_{238}{}^{238}U)$ throughout) and with age, because the same absolute bias becomes relatively less important in older samples. In modern seawater, the observed variation in $[^{234}U/^{238}U]$ is limited, with an average value of ca. 1.14 (Chen et al., 1986). Conversely, $[^{234}U/^{238}U]$ activity ratios in freshwater may be as high as 12 (Kronfeld et al., 1994; Vaks et al., 2020) which can make the raw $^{206}Pb/^{238}U$ dates inaccurate by as much as 4 Myr (Vermeesch et al., 2025). This problem is particularly acute for young freshwater carbonates such as those dated to produce climate and landscape reconstructions beyond ca. 600 ka, or to calibrate early hominin evolution (Pickering et al., 2019; Engel et al., 2020; Vaks et al., 2020). Here, the necessary correction may be as much as 80% of the measured $^{206}Pb/^{238}U$ date (Fig. 1a).

Corrections for initial $^{234}U/^{238}U$ disequilibrium can be implemented either by using a nominal, independently estimated initial $[^{234}U/^{238}U]$ value (e.g. average modern seawater, or local to regional groundwater composition), or by estimating it based on direct analyses of any residual disequilibrium in the sample. In freshwater samples, independent estimates are often not reliable as $[^{234}U/^{238}U]$ can be very variable locally (Kronfeld et al., 1994; Chen et al., 2016; Vaks et al., 2020), although there are some exceptionally well-characterised contexts (e.g. Chaldekas et al., 2021). The second method is in principle more robust and has been employed in a range of young samples (Wendt and Carl, 1985; Richards et al., 1998; Woodhead et al., 2006), commonly using a Monte Carlo approach that simultaneously finds a best-fitting date and initial $[^{234}U/^{238}U]$ (e.g. Pollard et al., 2023). Vermeesch et al. (2025) have shown theoretically that such corrections are robust for samples not older than about 1.5 Ma. Even so, as currently applied, this approach faces three major challenges: (1) analytically obtaining accurate $[^{234}U/^{238}U]_m$ values, (2) applying the measured $[^{234}U/^{238}U]_m$ values to the U/Pb analyses, (3) accurately modelling and propagating uncertainty. We will illustrate these issues with literature data from the Hoogland basal speleothem (South Africa) where the existing method has led to a particularly pronounced bias of the interpreted age (Fig. 1).

https://doi.org/10.5194/egusphere-2026-4403
Preprint. Discussion started: 7 August 2026

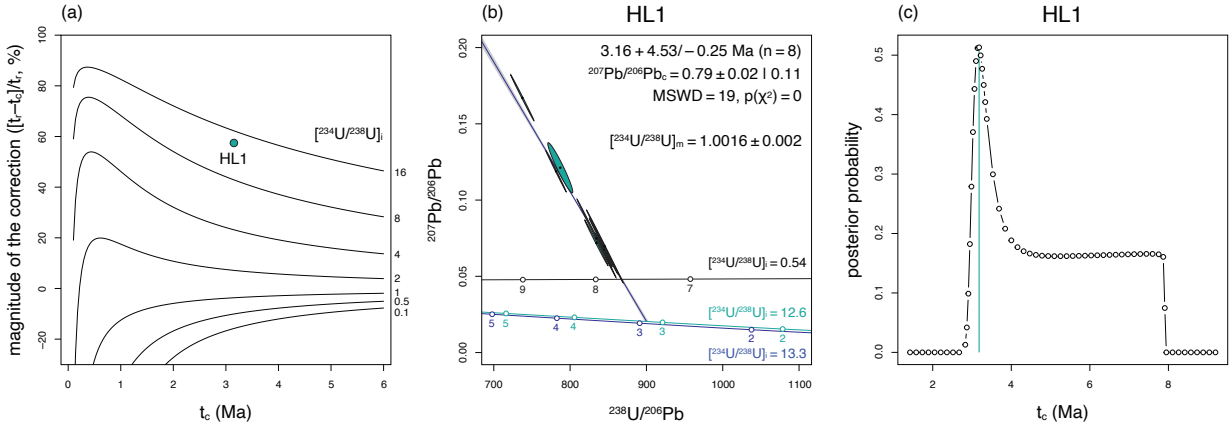

Figure 1: ^{234}U disequilibrium correction in young carbonates. (a) Nomogram of the relative magnitude of the correction vs. corrected date for different values of $[^{234}U/^{238}U]_i$; t_r is the uncorrected date, assuming secular equilibrium, t_c is the corrected date. (b) Disequilibrium-corrected U-Pb data of Pickering et al. (2019)'s Hoogland sample HL1, using a measured present-day $^{234}U/^{238}U$ activity ratio $[^{234}U/^{238}U]_m$ = 1.0016 with nominal 1‰ uncertainty (1σ); three concordia lines are shown, for the maximum likelihood solution (t_c = 3.16 Ma, corresponding to an inferred initial activity ratio $[^{234}U/^{238}U]_i$ = 12.6), the lower age limit (t_l = 2.91 Ma with $[^{234}U/^{238}U]_i$ = 13.3) and upper age limit (t_u = 7.69 Ma with $[^{234}U/^{238}U]_i$ = 0.54), respectively. (c) Posterior distribution of the corrected date, using a uniform prior for $[^{234}U/^{238}U]_i$ from 0 to 20; t_l and t_u correspond to the 2.5 and 97.5 percentiles of this distribution respectively; t_c is marked by a vertical line.

First, accurate analyses of small residual deviations from $^{234}U/^{238}U$ secular equilibrium are challenging due to the very large dynamic range of the analysis (238U/234U at equilibrium is ca. 18200; Hu et al., 2025). There is a range of related analytical effects that must be accurately corrected or monitored to obtain accurate $[^{234}U/^{238}U]_m$ values, including e.g. ion counter yield, dead time, non-linearity, as well as interferences or peak tailing on U masses. If the "natural" $^{238}U/^{235}U$ is used for mass bias correction, its value will also have an influence on accuracy, especially if it deviates (Stirling et al., 2007; Pollard et al., 2025) from the commonly assumed values (Steiger and Jäger, 1977; Hiess et al., 2012). Accurate corrections of $^{206}Pb/^{238}U$ dates using absolute $[^{234}U/^{238}U]$ activity values also critically depend on the accuracy of the employed ^{234}U decay constant. The decay constant directly affects the conversion from the measured $^{234}U/^{238}U$ ratio to activity ratio, but in analytical routines where $^{234}U/^{238}U$ is normalised to a certain "equilibrium ratio" in an old equilibrium material, it may also systematically affect the measured ratio itself. In the most recent recalibration, Hu et al. (2025) obtained a ^{234}U decay constant of 2.8215×10^{-6} a^{-1}, but the total range of ^{234}U decay constants employed in literature data is on the order of 5‰ (Table 1). For the Hoogland HL1 example in Fig. 1, Pickering et al. (2019) followed analytical methods of Woodhead et al. (2006) who reported using a decay constant of 2.835×10^{-6} a^{-1}, an average of those obtained by Lounsbury and Durham (1971) and De Bievre et al. (1971). Aligning the $[^{234}U/^{238}U]$ values for the Hoogland flowstone with the Hu et al. (2025) decay constant would require a reduction of their $[^{234}U/^{238}U]_m$ = 1.0016 to 0.9968 (Table 1), which would necessitate an

https://doi.org/10.5194/egusphere-2026-4403
Preprint. Discussion started: 7 August 2026

upward instead of downward correction to obtain the maximum likelihood $^{206}Pb/^{238}U$ date. This highlights how accurate $[^{234}U/^{238}U]_m$ is critical to the success of this approach.

Table 1: Conversion factors for legacy $[^{234}U/^{238}U]$ activity ratios to λ_{234} of Hu et al. (2025), assuming λ_{238} of Jaffey et al. (1971).

reference	λ_{234} (a^{-1})	$[^{234}U/^{238}U]$ conversion
Lounsbury and Durham (1971)	2.836×10^{-6}	0.9948
De Bievre et al. (1971)	2.834×10^{-6}	0.9956
Holden (1989)	2.8234×10^{-6}	0.9993
Ludwig et al. (1992)	2.8258×10^{-6}	0.9985
Cheng et al. (2000)	2.8263×10^{-6}	0.9983
Cheng et al. (2013)	2.8221×10^{-6}	0.9998
Varga et al. (2016)	2.830×10^{-6}	0.9969
Hu et al. (2025)	2.8215×10^{-6}	1

The second issue concerns appropriate matching of U/Pb and $[^{234}U/^{238}U]_m$ analyses. Many applications of the method have used a single blanket $[^{234}U/^{238}U]_m$ value per rock sample, applied across all aliquots of material analysed for U/Pb (Wendt and Carl, 1985; Richards et al., 1998; Woodhead et al., 2006; Pickering et al., 2019). The reason is that a precise $[^{234}U/^{238}U]$ analysis by solution MC-ICPMS (or by alpha spectrometry) requires a larger mass of material than a U/Pb one. However, in examples where multiple $[^{234}U/^{238}U]$ analyses were conducted within what was visually considered one speleothem layer (Walker et al., 2006; Dirks et al., 2010; Chaldekas et al., 2021), the $[^{234}U/^{238}U]_m$ data were not always equivalent within uncertainty. Thus, to account for any potential variability within a sample, the two analyses should ideally be obtained from the exact same volume of material, accompanied by a mathematical formulation of an aliquot-based disequilibrium correction.

Third, application of the disequilibrium correction to samples with residual $[^{234}U/^{238}U]_m$ close to 1 results in greatly expanded uncertainties. Recently, Vermeesch et al. (2025) showed that previously applied disequilibrium correction algorithms tended to underestimate uncertainty. For example, Pickering et al. (2019)'s $^{206}Pb/^{238}U$ Hoogland HL1 data define a trend in Tera-Wasserburg concordia space with a concordia intercept age of 7.407 ± 0.080 Ma (Fig. 1b). Using a single $[^{234}U/^{238}U]_m$ value of 1.0016 ± 0.001, this was corrected to 3.145 ± 0.243 Ma; i.e. a 60% reduction in age with a reported uncertainty of only 7.7% at 2σ. The corresponding initial $[^{234}U/^{238}U]$ activity ratio is 12.879 ± 1.728, an extreme value even for South African speleothems (Kronfeld et al., 1994). Vermeesch et al. (2025) introduced an alternative deterministic Bayesian uncertainty-estimation procedure. Applying this new algorithm to Pickering et al. (2019)'s $^{206}Pb/^{238}U$ data yields

https://doi.org/10.5194/egusphere-2026-4403
Preprint. Discussion started: 7 August 2026

the same date but a much larger, asymmetric 95% credible interval ranging from 2.94 to 7.69 Ma, corresponding to a range of 150% relative to the corrected date (Fig. 1c). Similarly, the 95% credible interval for $[^{234}U/^{238}U]_i$ ranges from 0.54 to 13.3. Clearly, this magnitude of analytical uncertainty on the $^{206}Pb/^{238}U$ dates limits the interpretability of the results.

A potential solution to the above problems is offered by the $^{207}Pb/^{235}U$ method which does not require a correction for initial $^{234}U/^{238}U$ disequilibrium (Vermeesch et al., 2025). The only long-lived intermediate daughter in the ^{235}U decay chain is ^{231}Pa, and $^{231}Pa/^{235}U$ disequilibrium is easily corrected once the extremely low solubility of Pa in water is considered [i.e., initial $[^{231}Pa/^{235}U]$ is safely assumed to be zero]. Even if this assumption is wrong, the maximum bias of an inaccurate ^{231}Pa correction is < 50 ka. The main disadvantage of the $^{207}Pb/^{235}U$ method (and the reason why the $^{206}Pb/^{238}U$ method has historically been more widely used for carbonate U–Pb dating) is the poorer analytical precision of the underlying mass-spectrometric measurements. Here we explore analytical implementations of the $^{207}Pb/^{235}U$ method in carbonates and use several reference materials and a Hoogland flowstone sample to demonstrate avenues to obtain precise and accurate $^{207}Pb/^{235}U$ dates.

2 Available analytical strategies

Carbonate samples suitable for U–Pb geochronology may have 0.1–100 ppm U, 0.1 ppb–10 ppm Pb, and generally negligible amounts of Th (Rasbury and Cole, 2009; Roberts et al., 2020). Most samples are heterogeneous in U/Pb ratios and concentrations, so the most promising domains need to be identified prior to analysis. This is generally achieved via preliminary LA-ICPMS analyses (mapping, line scans, spot analyses), phosphor imaging or XRF mapping (Rasbury et al., 2021), which is followed by final analysis. Alternatively, entire LA-ICPMS maps may be used to extract sub-domain dates in post-processing (Drost et al., 2018; Hoareau et al., 2021; Hoareau et al., 2025). Carbonates have much lower U/Pb ratios than U-rich accessory minerals, which generally precludes calculation of single-analysis dates; instead, we must rely on the isochron approach where a suite of cogenetic carbonate samples of variable U/Pb are used to calculate one common isochron date. The variations in U/Pb result from variations in the initial U content or in the amount of non-radiogenic (initial, or inherited) Pb between the analyses. For same-age data, greater variability in U/Pb is desired as it leads to better-defined isochron fits and smaller uncertainties on the isochron date.

For a $^{207}Pb/^{235}U$ isochron construction, we need to analyse ^{235}U, ^{207}Pb, and one of ^{208}Pb or ^{204}Pb which can both serve as time-independent proxies for initial Pb (Vermeesch et al., 2025). ^{204}Pb is a stable non-radiogenic isotope, while the measured ^{208}Pb will represent a mix of initial ^{208}Pb and radiogenic $^{208}Pb^*$ formed by the decay of ^{232}Th. However, with the low Th solubility in water and the long ^{232}Th half-life of ca. 14 Gyr, $^{208}Pb^*$ is effectively absent in most clean carbonate samples (Walker et al., 2006; Mason et al., 2013; Parrish et al., 2018; Mason et al., 2022); if that is not the case, it can be easily age-

https://doi.org/10.5194/egusphere-2026-4403
Preprint. Discussion started: 7 August 2026

corrected if ^{232}Th is analysed (Vermeesch, 2020). Thus, the analytical routine may also include ^{232}Th, as well as ^{206}Pb and ^{238}U to obtain an independent date for comparison.

In deciding which analytical method to use for U–Pb in carbonates, we need to consider (1) sampling size and (2) the non-radiogenic Pb masses (^{208}Pb or ^{204}Pb) that can be analysed accurately. Both factors will affect the precision and accuracy of the isochron date. Sampling size affects the variability of U/Pb ratio in a group of analyses; smaller sampling volumes should result in greater variability and greater spread along the isochron, likely leading to a more precise isochron fit (Fig. 2). Conversely, larger sampling sizes, even if they homogenise the obtained compositions to a greater degree, will result in smaller data-point uncertainties because they can be analysed at higher mass spectrometer intensities. In parallel, since we do not know a priori whether the sample is homogenous in its initial Pb isotopic composition, whether we use ^{208}Pb or ^{204}Pb as normalisation mass may affect precision and accuracy of the isochron fit.

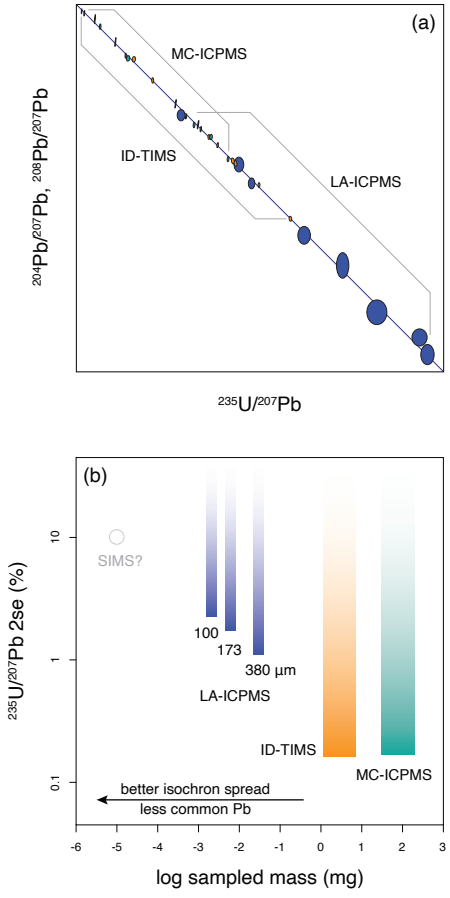

https://doi.org/10.5194/egusphere-2026-4403
Preprint. Discussion started: 7 August 2026

Figure 2: Schematic illustration of ^{207}Pb-^{235}U isochron data spread and precision expected from the main analytical methods in a hypothetical radiogenic carbonate sample. (a) Inverse isochron view (^{204}Pb- or ^{208}Pb-based) showing how sampling characteristics affect the position of data along the isochron. In situ data have the greatest spread and reach the highest U/Pb; solution data have more initial Pb. Their spread should roughly follow the sample mass. (b) Relationship between the achievable data-point uncertainty for $^{235}U/^{207}Pb$ and sampled mass (based on new and literature data). The precision of a theoretical SIMS analysis is a guess.

The available methods are mainly distinguished by how the sample is introduced into the mass spectrometer:

- solution-based methods

  Here, fragments of the sample are dissolved in acid, homogenised with an enriched isotope tracer, purified to isolate U and Pb, and analysed by high-precision mass spectrometry, either thermal ionisation mass spectrometry (TIMS, also called ID-TIMS to highlight the isotope dilution aspect) or multicollector inductively coupled plasma mass spectrometry (MC-ICPMS). A variety of this method that does not include U and Pb purification has also been applied to clean speleothem samples (Mason et al., 2022). Solution-based methods require relatively large samples to produce sufficiently high intensity and to avoid sensitivity to blank corrections related to sample handling and used reagents. Sample mass depends on U and Pb concentrations but has typically been in the range of 1–10 mg for ID-TIMS and 10s to 100s mg for MC-ICPMS. Because chemical separation is involved, for simplicity both methods are typically focused on U and Pb and do not include Th. ^{204}Pb and ^{208}Pb can be accurately analysed by ID-TIMS. ^{208}Pb is also easily analysed by MC-ICPMS; however, reliable ^{204}Pb analyses by ICPMS have been challenging due to a common interference from ^{204}Hg found in Ar gas (Hirata and Nesbitt, 1995; White et al., 2000). This effect is variable but historically has led to a distrust in ^{204}Pb analysed by ICPMS in small samples (Woodhead et al., 2006) and a focus on dates obtained in the $^{238}U/^{206}Pb$–$^{207}Pb/^{206}Pb$ space (Pickering et al., 2019) or using ^{208}Pb as the non-radiogenic Pb proxy (Mason et al., 2022; Vaks et al., 2025). The ability to analyse ^{204}Pb by ICPMS may improve by employing a reaction gas (Gilbert and Glorie, 2020) but this approach has not been widely adopted thus far. Consequently, ^{204}Pb normalisation of carbonate MC-ICPMS U–Pb results has been the exception (Dirks et al., 2010; Pickering et al., 2010) rather than the rule. Until ^{204}Pb analysis can be demonstrated to be accurate at the sample size of interest, MC-ICPMS applications must rely on ^{208}Pb as the proxy for non-radiogenic Pb.

- in situ methods

  In these methods a surface layer of the specimen is sampled with a laser beam (laser ablation (LA)-ICPMS) or an ion beam (secondary ion mass spectrometry, SIMS) to obtain highly spatially resolved compositions on much smaller sample volumes. The standard laser beam size for carbonate U–Pb geochronology ranges from 40 µm to >100 µm (0.3–2.5 µg sample mass)(Roberts et al., 2020) but it could be expanded up to over 350 µm (ca. 25 µg) in

https://doi.org/10.5194/egusphere-2026-4403
Preprint. Discussion started: 7 August 2026

some setups. In SIMS, beam sizes are generally smaller and sampled pits shallower, corresponding to sample masses in the ng range. While we are not aware of successful applications of SIMS to carbonate U–Pb geochronology, LA-ICPMS has recently become the main analytical tool for $^{206}Pb/^{238}U$ dating of older carbonates (Roberts et al., 2020). This technique is capable of quickly producing large amounts of data at lower data-point precision than offered by the solution methods. Due to the superior isochron spread resulting from smaller sampling sizes, it is however possible to obtain a good isochron fit for $^{206}Pb/^{238}U$ that may approach the precision of solution methods, particularly in the youngest samples. Finally, a typical LA-ICPMS setup generally cannot provide reliable ^{204}Pb data due to the Hg interference issue described above, so it must rely on ^{208}Pb normalisation, but the analytical routine can include Th, and it can accommodate other elements.

Our compilation in Fig. 2 shows that the best achievable precision on $^{235}U/^{207}Pb$ in a single analysis is on the order of 0.2% for the solution methods, and >1% for LA-ICPMS; this is a clear consequence of sampling size. However, the expected spread of data along the isochron is of equal or greater importance to isochron date calculation. LA-ICPMS facilitates avoiding contamination (by visual selection), shifting and expanding the range of data towards higher U/Pb, theoretically offering excellent isochron fits when datasets become large. Even so, the precision of in situ methods is ultimately limited by the used reference materials, while the long-term date reproducibility is unlikely to be better than 1–2% (Guillong et al., 2024). Solution methods are less flexible when it comes to eliminating contaminants, so their results tend to skew towards more common Pb-rich compositions. In detail, solution MC-ICPMS sampling sizes are 1–2 orders of magnitude larger than in ID-TIMS so it should be expected that the former delivers a more restricted spread of data. Thus, given the lower expected spreads at similar data-point uncertainties (Fig. 2) there seems to be no advantage of using solution MC-ICPMS over ID-TIMS, especially considering that ^{204}Pb may be difficult to analyse by ICPMS. Solution MC-ICPMS remains an acceptable analytical tool for the job (e.g. Vaks et al., 2020; Vaks et al., 2025), but without ^{204}Pb, it remains inferior to ID-TIMS which can provide accurate ^{204}Pb data.

Taking these variables into account, we conclude that $^{207}Pb/^{235}U$ carbonate geochronology is best conducted by LA-ICPMS for quick, high-throughput analyses at lower precision, or by ID-TIMS for the most precise and accurate, but labour-intensive analyses. Below we describe attempts to optimise analyses using the two methods and demonstrate their suitability for the task. First, we provide new and reprocessed ID-TIMS data to explore the potential for the most precise $^{207}Pb/^{235}U$ results. We then explore adaptations of the LA-ICPMS analytical strategy that allow us to produce accurate in situ isochron $^{207}Pb/^{235}U$ dates at a useful precision.

https://doi.org/10.5194/egusphere-2026-4403
Preprint. Discussion started: 7 August 2026

3 Material and methods

3.1 Samples

We used carbonate reference materials: the ca. 3 Ma ASH15 (D+K) speleothem (Nuriel et al., 2021) and the ca. 322 Ma RA138 marine calcite (Guillong et al., 2024). While they were not specifically analysed to obtain $^{207}Pb/^{235}U$ dates, the existing ID-TIMS data for these samples could be reprocessed to provide $^{207}Pb–^{235}U$ isochrons and $^{208}Pb/^{204}Pb$ ratios. We also newly analysed a South African speleothem from the Hoogland paleocave (X4); this sample, previously dated by ID-TIMS by Hopley et al. (2019), comes from the same basal flowstone as sample HL1 dated by MC-ICPMS by Pickering et al. (2019) and should be directly comparable (Fig. 1). For laser ablation analyses, we additionally used the ca. 43 Ma calcite breccia AUG-B6 (Pagel et al., 2018).

3.2 ID-TIMS

Hoogland speleothem X4 was cut to yield a 2 cm wide stick perpendicular to layering, which was polished and scanned on a desktop scanner. LA-ICPMS analyses were then conducted to obtain compositional profiles across the polished sample surface (Fig. 3). The layer with the highest U/Pb was isolated from the stick with a diamond wire saw to yield a 2 mm thick slice (Fig. 3). The slice was then subdivided into sub-mm pieces with a scalpel. The focus was on internal domains of the slice, avoiding outside surfaces previously exposed to saws and the related contamination. Pieces suitable for analysis were chosen in the mass range of 1.5–6 mg and were, where possible, free of visible surface impurities of non-carbonate material. Before washing and dissolution, they were weighed on a microbalance.

Single carbonate pieces were sonicated in acetone and ultrapure water, then transferred to individual 3 ml screw-top PFA vials. After an additional rinse in ultrapure water, they were dissolved in ca. 150 µl 6 M HCl. Following dissolution, 5–9 mg of the EARTHTIME $^{205}Pb–^{233}U–^{235}U$ (ET535) tracer solution (Condon et al., 2015; McLean et al., 2015) was added to each vial. Samples were equilibrated with the tracer for 2 h on a 100 ºC hotplate and subsequently dried to chloride salts. For U–Pb separation, samples were redissolved in 1 M HBr and loaded onto 50 µl columns filled with AG1-X8 ion exchange resin. Pb and U were isolated from the solutions in a two-step, HBr and HCl-based ion exchange procedure. Uranium and Pb fractions were collected in separate 7 ml PFA vials and dried down with trace H_3PO_4.

https://doi.org/10.5194/egusphere-2026-4403
Preprint. Discussion started: 7 August 2026

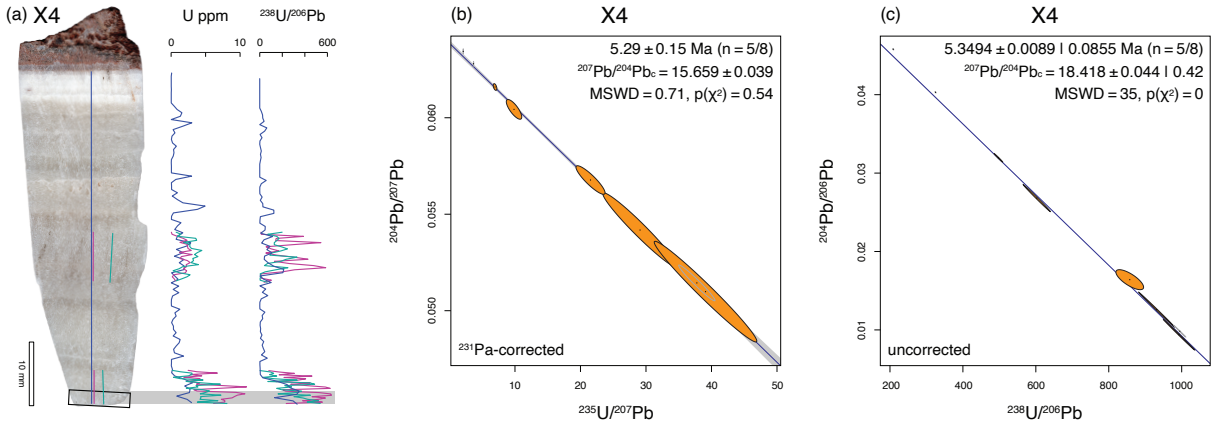

Figure 3: ID-TIMS U–Pb geochronology of Hoogland basal flowstone X4. (a) Sample scan and location of traverses analysed for U concentration and U/Pb ratio. Black box marks the slice selected for ID-TIMS analyses. (b) ^{207}Pb–^{235}U isochron corrected with initial [$^{231}Pa/^{235}U$] = 0. (c) ^{206}Pb–^{238}U isochron uncorrected for U-series disequilibria.

Samples were then dissolved in a silica-gel emitter (modified from Gerstenberger and Haase, 1997) and loaded on single, outgassed, zone-refined Re filaments for analysis on a Thermo Triton Plus thermal ionisation mass spectrometer (TIMS). Both Pb and UO_2 analyses were performed using static multicollection in Faraday cups connected to 10^{13} Ω resistors (von Quadt et al., 2016) except cases of low Pb intensity where ^{204}Pb was collected in the axial secondary electron multiplier. Electronic Faraday baselines were acquired for 1 h twice daily. $^{18}O/^{16}O$ in the UO_2 analyses was determined online by monitoring mass 272 (Wotzlaw et al., 2017) when sufficient intensity was available, otherwise a value of $^{18}O/^{16}O = 0.00205 \pm 2$ (1 s) was applied to correct for interferences.

All isotopic ratios were processed in Tripoli (Bowring et al., 2011) and a spreadsheet following the equations of Schmitz and Schoene (2007) modified to include $^{208}Pb/^{204}Pb$ quantification. Instrumental mass fractionation in Pb isotope analyses was corrected with a value of 0.072 ± 0.025 (1σ) %/amu based on a long-term compilation of Faraday Pb analyses performed with a double-Pb spike. For U, instrumental mass fractionation was determined using the known $^{233}U/^{235}U$ of the tracer and assuming that the samples had $^{238}U/^{235}U$ of 137.818 ± 0.045 (2s; Hiess et al., 2012). Departures in $^{238}U/^{235}U$ of up to 0.5‰ have been documented in some speleothems (Pollard et al., 2025) but even such extreme values have no discernible effect on U–Pb sample age at the current precision level. Measured isotope ratios were corrected for laboratory blank whose mass and isotopic composition were estimated based on analyses of 12 total procedural blanks run alongside unknowns, yielding a Pb blank mass of 0.74 ± 0.32 (1σ) pg with a composition of $^{206}Pb/^{204}Pb$ = 18.28 ± 1.3%, $^{207}Pb/^{204}Pb$ = 15.66 ± 0.8%, and $^{208}Pb/^{204}Pb$ = 38.11 ± 1.2%, (all 1σ), and U blank of 0.39 ± 0.07 (1σ) pg (assuming isotopic composition identical to sample). Data pertinent to $^{207}Pb/^{235}U$ geochronology are shown in Table 2 while all sample isotopic compositions are reported in the

https://doi.org/10.5194/egusphere-2026-4403
Preprint. Discussion started: 7 August 2026

supplement. Isochron ages were calculated using decay constants of Jaffey et al. (1971) for ^{235}U and Audi et al. (2003) for ^{231}Pa. Corrections for ^{231}Pa disequilibrium assumed initial [^{231}Pa/^{235}U] = 0.

3.3 LA-ICPMS

Laser ablation analyses were performed using an ASI RESOlution LR 193 nm excimer ArF laser ablation system coupled to a Thermo Element XR single-collector sector field ICP-MS following a workflow modified from Guillong et al. (2024) collecting ^{202}Hg, ^{204}Pb, ^{206}Pb, ^{207}Pb, ^{208}Pb, ^{232}Th, ^{235}U, and ^{238}U. For LA-ICPMS data, we use the inverse ^{235}U/^{207}Pb–^{208}Pb/^{207}Pb isochron construction (Fig. 2) so the primary focus is on accurate analyses of ^{207}Pb, ^{208}Pb, and ^{235}U. Preliminary analyses showed that the standard 100 µm spot size leads to unacceptably large uncertainties for the youngest samples (e.g. ASH15) so we adopted the largest available spot size of 380 µm to maximise ion yield. We used static spot ablation at 5 Hz and an energy density of ~2 J/cm^2. To improve precision for small ion beams, the counting times were extended to 100 ms for ^{207}Pb, to 50 ms for ^{208}Pb, and to 20 ms for ^{235}U, while other isotopes were analysed for 11 ms, resulting in a sweep time of 0.243 s.

All isotopic ratios and intensities were corrected following an adaptation of the standard procedure used in ^{206}Pb/^{238}U carbonate geochronology (Roberts et al., 2017; Guillong et al., 2020). Initial processing was done in Iolite 4 (Paton et al., 2011) and included selection of integration intervals, gas blank subtraction, and the correction of the ^{235}U/^{207}Pb ratio for laser-induced elemental fractionation using the U–Pb data reduction scheme (Paton et al., 2010) with NIST SRM 614 glass as the primary reference material. Further treatment was implemented in an Excel spreadsheet. First, fractionation-corrected ^{235}U/^{207}Pb ratios were corrected for drift using NIST614. Raw ^{208}Pb/^{207}Pb was calculated from the two intensities (ratio of intensity) and corrected to the known value for NIST614 (^{208}Pb/^{207}Pb = 2.4125 estimated from values available in GeoReM, Jochum et al. (2005)). Corrected ratios for RA138 were then used to calculate a ^{207}Pb–^{235}U isochron date; the comparison of this date with the isochron date obtained by ID-TIMS gave a correction factor applied to all unknown ^{235}U/^{207}Pb ratios throughout the sequence. Propagated uncertainties include those resulting from counting statistics and from the RA138 correction, but do not include systematic uncertainties which are likely >1.5 % as determined for ^{206}Pb/^{238}U dates in RA138 (Guillong et al., 2024). Detailed description of the instrumental setup and methodology used, and all results are included in the supplement.

4 Results and discussion

4.1 ID-TIMS geochronology

Our new (Table 2) and reprocessed ID-TIMS results demonstrate the ability of this method to generate highly precise ^{207}Pb/^{235}U dates. For ID-TIMS data, we use the inverse ^{235}U/^{207}Pb–^{204}Pb/^{207}Pb isochron construction (Fig. 3). The Hoogland

https://doi.org/10.5194/egusphere-2026-4403
Preprint. Discussion started: 7 August 2026

X4 sample returned ^{207}Pb–^{235}U isochron dates of 5.29 ± 0.15 Ma (filtered, n = 5/8, details of filtering in section 4.3 below) and 5.35 ± 0.13 Ma (n = 8/8). Both dates are consistent with the ID-TIMS ^{207}Pb–^{235}U isochron date of 4.9 ± 1.9 Ma of Hopley et al. (2019) obtained on the same sample X4, and are indistinguishable from our uncorrected ^{206}Pb–^{238}U isochron date of 5.349 ± 0.085 Ma (n = 5/8), indicating that initial $^{234}U/^{238}U$ disequilibrium was likely negligibly small. Our X4 dates are also consistent with the Tera-Wasserburg intercept date of Pickering et al. (2019) for the same speleothem when corrected using the Vermeesch et al. (2025) algorithm (Fig. 1c), but not when the original correction is applied.

Table 2: New ID-TIMS $^{207}Pb/^{235}U$ data for Hoogland speleothem sample X4.

Sample	Composition							Isotope ratios						
	mass (mg)	U (ppm)	Pb (ppm)	1/Pb	±2σ	Pb^*/Pb_i	Pb_i (pg)	$^{208}Pb/^{204}Pb$	±2σ	$^{235}U/^{207}Pb$	±2σ %	$^{204}Pb/^{207}Pb$	±2σ %	rho
X4-1	**1.46**	**1.50**	**0.005**	**185**	**9**	**0.26**	**6.2**	**38.59**	**0.17**	**9.855**	**9.78**	**0.060434**	**0.69**	**-0.778**
X4-2	**1.70**	**2.33**	**0.004**	**268**	**16**	**0.86**	**3.4**	**38.35**	**0.26**	**29.093**	**15.92**	**0.054180**	**2.90**	**-0.971**
X4-3	**3.84**	**1.35**	**0.002**	**547**	**31**	**1.24**	**3.1**	**38.57**	**0.30**	**39.091**	**16.38**	**0.050987**	**4.18**	**-0.981**
X4-4	**2.01**	**2.34**	**0.011**	**89**	**2**	**0.18**	**19.2**	**38.38**	**0.09**	**6.959**	**3.23**	**0.061593**	**0.23**	**-0.477**
X4-5	3.09	2.14	0.031	32	0	0.04	92.4	37.91	0.08	2.101	0.70	0.063439	0.17	0.107
X4-7	5.78	2.37	0.003	310	6	1.16	8.6	38.07	0.13	37.766	6.01	0.051440	1.47	-0.975
X4-8	6.00	2.41	0.021	48	0	0.08	114.5	38.13	0.08	3.673	0.56	0.062797	0.16	0.120
X4-11	**2.93**	**1.98**	**0.004**	**259**	**9**	**0.60**	**7.1**	**38.62**	**0.16**	**21.531**	**8.42**	**0.056773**	**1.07**	**-0.894**

All sample ratios and concentrations are corrected for fractionation, spike, and blank. Pb* and Pb_i represent radiogenic and initial Pb, respectively.
Analyses in bold type have coherent $^{208}Pb/^{204}Pb$ ratios and were included in the "filtered" isochron construction.

Reprocessed RA138 data (Fig. 4) gave ^{207}Pb–^{235}U isochron dates of 324.0 ± 2.3 Ma (n = 15/21) and 323.0 ± 3.9 Ma (n = 21/21), both indistinguishable from the uncorrected Tera-Wasserburg intercept dates of 321.99 ± 0.65 Ma (n = 17/21) and 320.8 ± 1.3 Ma (n = 21/21) presented by Guillong et al. (2024). This result is also consistent with the uncorrected ^{206}Pb–^{238}U isochron dates for the same data of 321.4 ± 1.4 Ma (n = 15/21) and 321.4 ± 1.1 Ma (n = 21/21). Reprocessed ASH15 data returned ^{207}Pb–^{235}U isochron dates of 3.084 ± 0.056 Ma (n = 35/36) and 3.086 ± 0.056 Ma (n = 36/36), which is older than the uncorrected Tera-Wasserburg intercept date of 2.965 ± 0.011 Ma (n = 35/36, Nuriel et al. (2021)) and the uncorrected ^{206}Pb–^{238}U isochron date of 2.974 ± 0.015 Ma (n = 35/36) but consistent with minor amounts of initial disequilibrium determined in Ashalim speleothems by Vaks et al. (2010). In the three presented cases, the uncertainty of ^{207}Pb–^{235}U isochron dates is a factor of 1.5–6 larger than that of the respective uncorrected ^{206}Pb–^{238}U isochron or Tera-Wasserburg concordia intercept date, but in each case the dispersion of ^{207}Pb–^{235}U data is consistent with a single age population, while ^{206}Pb–^{238}U data are overdispersed.

https://doi.org/10.5194/egusphere-2026-4403
Preprint. Discussion started: 7 August 2026

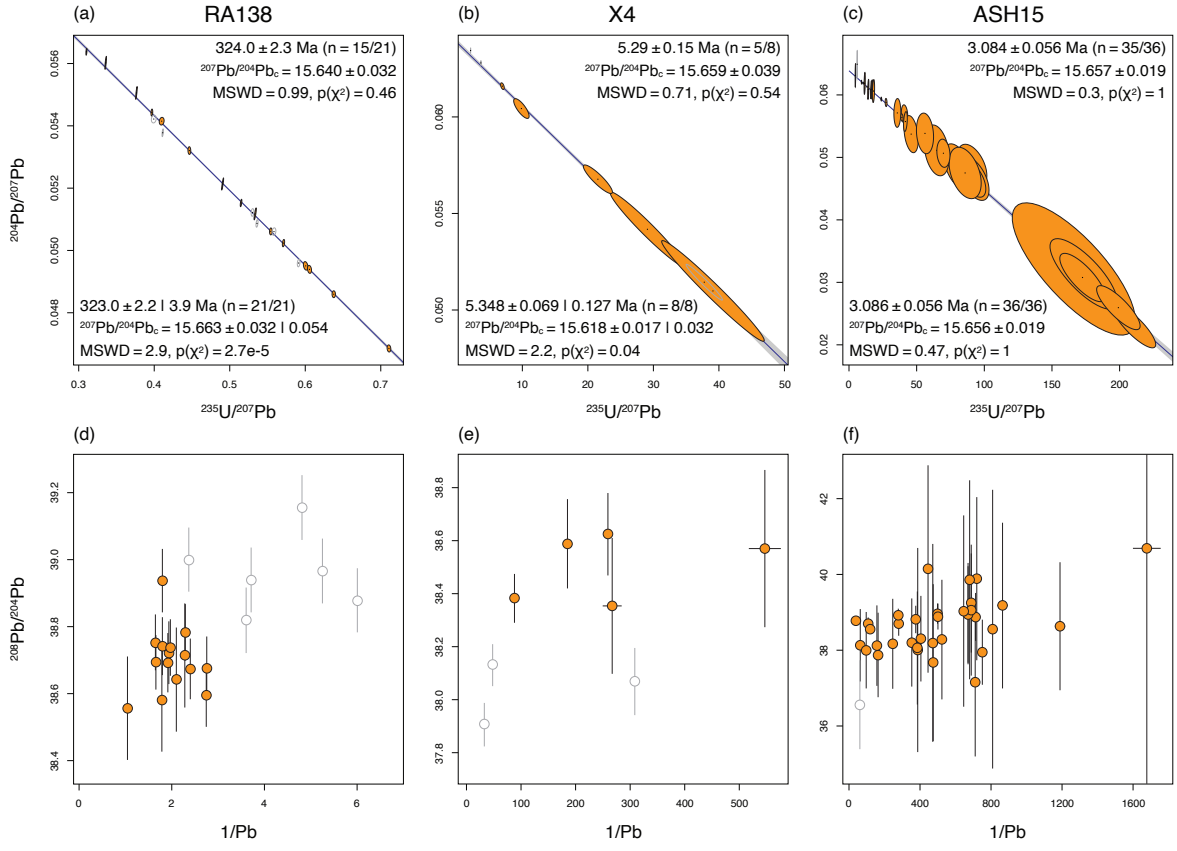

315 **Figure 4: Utility of $^{208}Pb/^{204}Pb$ in carbonates as a tracer of contamination, and its effect on age interpretation. (a–c) ^{208}Pb-filtered and unfiltered, ^{231}Pa-corrected ID-TIMS ^{207}Pb–^{235}U isochron dates for RA138, X4, and ASH15. (d–f) corresponding measured $^{208}Pb/^{204}Pb$ vs. 1/(Pb ppm) systematics and suggested exclusion of outliers.**

4.2 Pb blank correction in ID-TIMS

320 At the sample sizes employed here, the key variable governing the size and shape of uncertainty envelopes in the ^{207}Pb–^{235}U isochron diagram is the Pb blank correction. This is because in some cases sample ^{207}Pb is low enough that a large fraction of the measured ^{207}Pb comes from the laboratory blank. In most cases, the blank Pb isotopic composition is indistinguishable from the composition of the initial Pb in the sample (there may be some exceptions; see Szymanowski et al., 2025 for a compilation of TIMS lab Pb blank compositions). Consequently, the blank correction will shift data along the isochron and
325 away from the common Pb intercept, expanding data-point uncertainty and turning positive error correlations into strongly negative ones. In cases where the two compositions are different, the correction might add scatter to the data, which highlights the importance of correctly accounting for blank mass and isotopic composition. In the dataset presented here, the

https://doi.org/10.5194/egusphere-2026-4403
Preprint. Discussion started: 7 August 2026

mass ratio of sample to blank Pb was generally <100 (and often <10) in ASH15 and X4, and it was on the order of 100–1000 for RA138. Young or small samples similar to ASH15 or X4 may be very sensitive to the blank correction parameters. For example, X4 has relatively more correlated errors than ASH15 at similar sample sizes and U/Pb ratios (Fig. 4), which is a consequence of a 3x larger relative uncertainty on the Pb blank mass used in reducing the X4 data. In cases of significant sensitivity, it might be worthwhile to increase the sample size to improve data-point uncertainties; however, this may come at the cost of decreased spread in the isochron diagram. Old/radiogenic samples such as RA138 will be less affected by blank corrections but such considerations are an important part of planning how much material to dissolve for ID-TIMS analyses.

4.3 Identifying contamination in U–Pb results with $^{208}Pb/^{204}Pb$

In carbonate U–Pb geochronology, sample characteristics dictate that we rely on the isochron approach, where a suite of cogenetic samples of variable U/Pb are used to calculate one isochron date. The variations in (blank-corrected) U/Pb and Pb/Pb ratios, and the position along the isochron, result from variable mixing between U-bearing domains of the sample containing radiogenic Pb, and initial Pb-bearing domains. By definition, an isochron is a mixing line between domains of the same age and the same, single initial Pb component. It follows that for a sample of homogeneous age, a real isochron can only accommodate mixing with one isotopic endmember of initial Pb. A violation of this requirement may manifest in the form of obvious excess scatter of data about the isochron but it may also bias the date in ways that are invisible to common statistics describing the quality of isochron fits such as MSWD. Thus, it would be advantageous to isochron age determination if extraneous initial Pb components could be identified and excluded from calculation, thereby satisfying the basic principle of the isochron and improving the accuracy of age interpretation.

In Fig. 4 we illustrate a method to use the measured (blank-corrected) $^{208}Pb/^{204}Pb$ as a provenance index of initial Pb that expands upon the suggestion of Engel et al. (2019). ^{204}Pb is a stable, non-radiogenic isotope, while the measured ^{208}Pb will represent a mix of initial ^{208}Pb and the generally negligible radiogenic $^{208}Pb^*$. In Th-free carbonates (as well as any $^{208}Pb^*$-corrected Th-rich samples), both ^{208}Pb and ^{204}Pb should remain invariant after the closure of the system and so a sample's $^{208}Pb/^{204}Pb$ ratio should only depart from the initial value in cases of mixing with extraneous Pb sources. An anomalous $^{208}Pb/^{204}Pb$ of an analysed aliquot is a reason to suspect that the aliquot violates the initial Pb homogeneity requirement of the isochron approach, which may introduce bias to its $^{204}Pb/^{207}Pb$ and $^{235}U/^{207}Pb$ systematics.

To apply any exclusion criteria, we need enough analyses to identify any trends in the data, while the data-point uncertainties need to be sufficiently small to distinguish trends with confidence. The simplest approach would be to eliminate statistical outliers in $^{208}Pb/^{204}Pb$ (Engel et al., 2019), but ideally we may strengthen the interpretations by developing an understanding of the geochemistry of the possible mixing endmembers. These may include, for example, detrital material included in the sampled volume whose Pb isotopic composition may be known or estimated, younger alteration, contamination at the

https://doi.org/10.5194/egusphere-2026-4403
Preprint. Discussion started: 7 August 2026

sampling site or in processing. Detrital components of different age may have very different Pb isotopic compositions that are to some extent predictable.

We plot $^{208}Pb/^{204}Pb$ in our three ID-TIMS datasets against the reciprocal of Pb concentration, which can visualise straight-line mixing trends (Fig. 4). We suggest a possible approach to data filtering that is not exhaustive; it is only meant to illustrate the potential of the method. In the case of Hoogland speleothem X4, we find five indistinguishable main-group analyses and three that are trending toward a high-Pb, low-$^{208}Pb/^{204}Pb$ endmember. The Hoogland cave was developed within the Archean–Proterozoic Malmani Subgroup dolomite; similar old U-poor dolomites in the Transvaal craton can have $^{208}Pb/^{204}Pb$ values as low as 35.0–35.6 (Bau et al., 1999). Low $^{208}Pb/^{204}Pb$ values thus likely represent contamination with similar old, non-radiogenic material. In contrast, among the data for RA138 one can identify a low-Pb, high-$^{208}Pb/^{204}Pb$ endmember that may be more easily explained with a younger (i.e. not Archean) rock contaminant or a modern lab-derived component. The analyses of RA138 were conducted on powders resulting from the drilling of one specific type of marine cement out of a total of four carbonate generations in the rock (Guillong et al., 2024); it is conceivable that some analyses may have included a fraction of Pb derived from a different carbonate generation. The ASH15 data come with large uncertainties on $^{208}Pb/^{204}Pb$ which are expected from small samples of initial Pb-poor carbonate; we only identify one potential high-Pb, low-$^{208}Pb/^{204}Pb$ outlier.

Applying our exclusion criteria results in improving the goodness of fit of the isochrons for RA138 and X4, with a negligible effect on ASH15 (Fig. 4). Thus, the suggested approach appears promising for identifying data skewing the $^{204}Pb/^{207}Pb$–$^{235}U/^{207}Pb$ systematics that may go otherwise unnoticed, and it provides a geology-based outlier detection tool that is superior to outlier rejection based purely on poor statistical fit. While this approach is helpful, it should be used with care in considering appropriate endmembers and avoiding 'cherry picking' purely for the sake of improving isochron statistics (Vermeesch, 2026). Finally, the variability of $^{208}Pb/^{204}Pb$ illustrated here has two important consequences for selecting the optimal analytical strategy for $^{207}Pb/^{235}U$ geochronology: (1) variations in ^{208}Pb in Th-poor carbonates imply that ^{208}Pb is not ideal as a normalisation isotope for ^{207}Pb–^{235}U isochrons, (2) analytical setups that can produce precise and accurate ^{204}Pb data (ID-TIMS, rarely ICPMS) offer a big advantage over those that do not (most literature solution and laser ablation ICPMS data).

4.4 LA-ICPMS geochronology

For LA-ICPMS, we use the inverse $^{235}U/^{207}Pb$–$^{208}Pb/^{207}Pb$ isochron construction (Fig. 5). In the three investigated samples, data describe clear linear arrays, apart from several anomalous analyses of ASH15 which will be discussed below. We can evaluate the accuracy of the LA-ICPMS data by reference to ^{207}Pb–^{235}U ID-TIMS isochrons in Fig. 4. The $^{207}Pb/^{235}U$ data for AUG-B6 are slightly overdispersed (MSWD = 2.6) yielding an isochron date of 47.0 ± 3.5 Ma (n = 14/15, excluding one

https://doi.org/10.5194/egusphere-2026-4403
Preprint. Discussion started: 7 August 2026

low-intensity analysis). AUG-B6 does not have an ID-TIMS reference age, but its age is expected to be ca. 43 ± 1 Ma based on LA-ICPMS $^{206}Pb/^{238}U$ data (Pagel et al., 2018). Results for X4 (5.09 ± 0.26 Ma, MSWD = 1.2, n = 30/30) are in excellent agreement with the ID-TIMS ^{207}Pb–^{235}U isochron date of 5.29 ± 0.15 Ma. Interestingly, the $^{235}U/^{207}Pb$ ratios returned by LA-ICPMS for X4 (ranging from 45 to 140) were all larger than those obtained for solutions (2–39), which underscores the capacity of laser ablation sampling to avoid visible contamination. Finally, data for ASH15 were slightly overdispersed (MSWD = 3.5, n = 50/50) and resulted in an isochron date of 3.04 ± 0.25 Ma, again in excellent agreement with the ID-TIMS date (Fig. 4). Here, the range of U/Pb ratios was more restricted than for solution data, suggesting that common Pb in this sample is not hosted in any major 'hotspots' (that may be more easily picked up by solution analyses but avoided by laser sampling) but that it is distributed within the lattice. The precision of our LA-ICPMS ^{207}Pb–^{235}U isochron dates is 3–6 times lower than the corresponding Tera-Wasserburg concordia intercept dates, which is comparable to the result obtained for ID-TIMS.

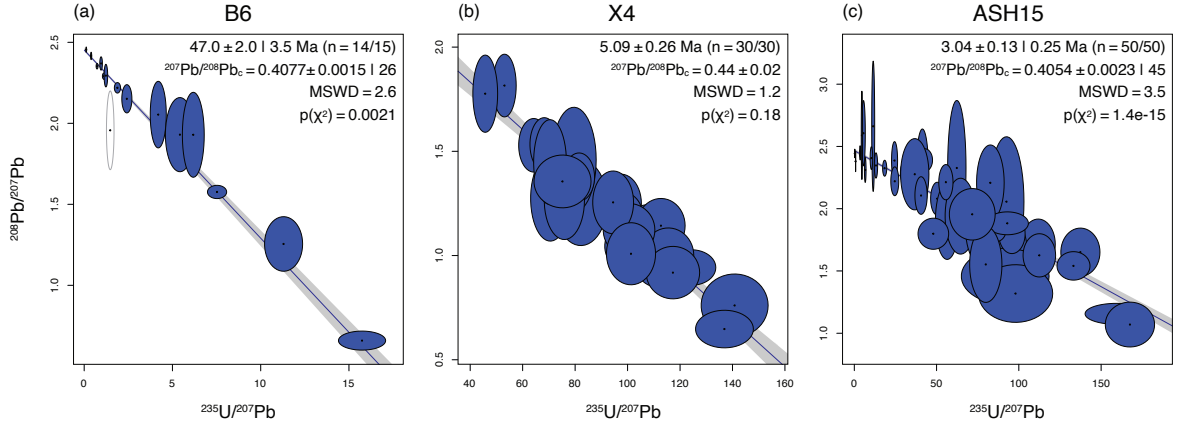

Figure 5: LA-ICPMS results for B6, X4, ASH15 obtained with the $^{207}Pb/^{235}U$ method using a 380 µm diameter laser spot. All isochron dates are disequilibrium-corrected with initial $[^{231}Pa/^{235}U] = 0$.

The consistency of our LA-ICPMS data with the ID-TIMS isochron dates for X4 and ASH15 suggests that at least in these two cases, using ^{208}Pb as the numerator in the y-axis ratio does not have major adverse effects. One explanation is that there was no heterogeneity in $^{208}Pb/^{204}Pb$ at the scale of laser sampling, another possibility is that it was masked by lower analytical precision. Notwithstanding the general consistency of isochron dates, the relatively large scatter of the LA-ICPMS ASH15 data suggests that the ASH15 sample analysed by LA-ICPMS may have some amount of heterogeneity in the initial Pb isotopic composition that was undetectable in the ID-TIMS $^{208}Pb/^{204}Pb$ data due to large uncertainties in this Pb-poor sample (Fig. 4). In fact, this is supported by ^{206}Pb–^{238}U data which display two distinct arrays in the Tera–Wasserburg diagram with very different apparent common Pb intercepts (Fig. 6). Some of the data in the lower-$^{207}Pb/^{206}Pb$ array are also

https://doi.org/10.5194/egusphere-2026-4403
Preprint. Discussion started: 7 August 2026

enriched in Th up to 1 ppb, suggesting a detrital component. This is in contrast to previous LA-ICPMS data on ASH15 (Nuriel et al., 2021) which scattered around a single isochron, and may be specific to the newly mounted material prepared specifically for this study utilising large laser spots. Irrespective of the exact reason, this behaviour is an opportunity which may be used in a fashion similar to $^{208}Pb/^{204}Pb$ filtering: identifying outliers in Tera-Wasserburg space or in Th concentration which may contribute to improving the $^{207}Pb/^{235}U$ isochron date interpretation. In the case of ASH15, excluding 12 low-$^{207}Pb/^{206}Pb$ data points results is no improvement of the scatter; however, this illustrates the benefit of analysing $^{206}Pb/^{238}U$ as part of the LA-ICPMS routine.

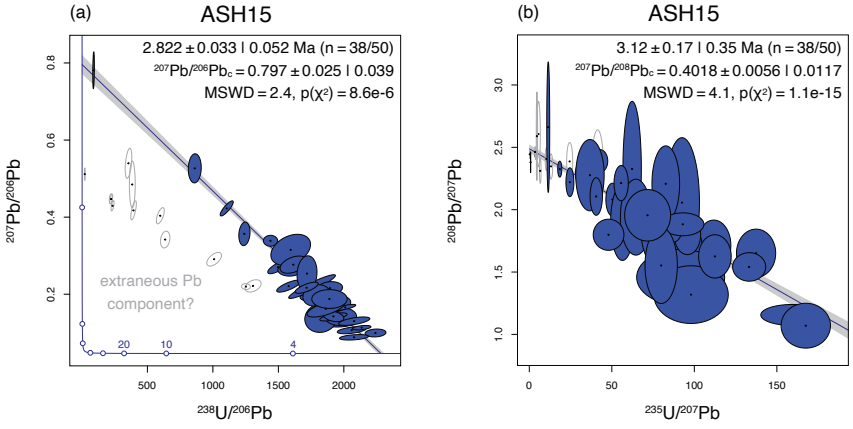

Figure 6: Filtered ASH15 LA-ICPMS results. (a) Tera-Wasserburg diagram illustrating an array of data projecting towards an anomalous $^{207}Pb/^{206}Pb$ ratio. (b) Filtered ^{207}Pb–^{235}U isochron excluding 12 points identified as outliers in panel (a).

The main challenge encountered in implementing LA-ICPMS carbonate $^{207}Pb/^{235}U$ geochronology in young samples was the low signal intensity for all involved isotopes, which may make the analyses particularly sensitive to outlier ("spike") rejection. Such spikes in the time-resolved signal are often expressed as increased counts for a single mass spectrometer sweep, and they likely reflect the detection of single larger particles mobilised from the ablation cell, sample or transfer tubing. The spikes are not representative of the sample composition, but they may skew a low (10s to 100s cps) intensity signal in a major way, creating biases in the resulting ratios. In this case, we performed spike elimination on the ^{208}Pb and ^{207}Pb signals separately (2 SD outlier rejection) before calculating a ratio from the means of the two signals (ratio of intensities) to increase chances of success compared to doing this using the time-resolved $^{208}Pb/^{207}Pb$ signal (mean of ratios). However, ten analyses in the ASH15 dataset were particularly spiky, so the Iolite routine could not remove the spikes correctly, leading to large biases to the $^{208}Pb/^{207}Pb$ ratio. This was not a problem for X4, which was measured at similar

https://doi.org/10.5194/egusphere-2026-4403
Preprint. Discussion started: 7 August 2026

<1000 cps intensities, suggesting that this behaviour is sample-specific. In ASH15, this affected a fraction of analyses which could be excluded from consideration, but any implementations of this method should carefully monitor for this effect.

5 Conclusions

We have shown here why it is important to turn to $^{207}Pb/^{235}U$ geochronology to date carbonates whose initial $^{234}U/^{238}U$ disequilibria are unconstrained – i.e., all carbonates beyond ca. 1.5 Ma. We have then demonstrated that such analyses are feasible by both solution-based and in situ techniques, arguing that ID-TIMS and LA-ICPMS are the best tools for this application. ID-TIMS offers the ultimate accuracy through the use of an isotopic tracer, and it is the most precise technique available, particularly for older radiogenic samples. Instead, optimised LA-ICPMS can quickly provide large quantities of data that result in comparable isochron date precision in some very young samples, but its precision is ultimately limited to several percent. A key factor to consider in choosing the analytical method is contamination with extraneous Pb components, which may bias the obtained date. While ID-TIMS provides generally precise analyses of ^{204}Pb than can be used to filter the data using $^{208}Pb/^{204}Pb$, LA-ICPMS (and solution MC-ICPMS) may not offer this option. Deviations seen in the corresponding Tera-Wasserburg data space, in Th content or other isotopic space may fill this role for some (LA-)ICPMS datasets. In any case, collecting additional compositional information (such as trace elements, e.g. Woodhead et al., 2012) from the sampled material might be a worthwhile effort leading to improved accuracy of age interpretation. This could involve adding more elements to the LA-ICPMS analytical routine or analysing trace elements in an aliquot of the dissolved material.

Since in many cases that require U–Pb geochronology initial $^{234}U/^{238}U$ disequilibria are unconstrained or impossible to correct while maintaining useful precision, we recommend the $^{207}Pb/^{235}U$ method for all applications where meteoric water was involved in rock formation. While we do not find evidence for large initial disequilibria in either of the speleothem datasets presented here, measurements of groundwaters and of young speleothems globally provide evidence that the disequilibria may be overwhelming for $^{206}Pb/^{238}U$ geochronology. Marine carbonates, where seawater $[^{234}U/^{238}U]$ is relatively better constrained, might be more permissive to the use of $^{206}Pb/^{238}U$ geochronology if appropriate uncertainty is assigned to the initial $[^{234}U/^{238}U]$ value to account for past seawater changes (Chutcharavan et al., 2018); however, high-accuracy applications are still better served by the $^{207}Pb/^{235}U$ method.

Data availability

All original and reprocessed data presented in the paper are available in the supplement.

https://doi.org/10.5194/egusphere-2026-4403
Preprint. Discussion started: 7 August 2026

Author contributions

DS and MG developed the analytical methods and conducted the analyses. DS recalculated previously published ID-TIMS data. PV developed algorithms for Bayesian disequilibrium correction and uncertainty propagation and reassessed existing analytical data for the Hoogland speleothem. PH provided sample X4. DS prepared the manuscript with contributions from all co-authors.

Competing interests

At least one of the (co-)authors is a member of the editorial board of *Geochronology*. The authors have no other competing interests to declare.

Disclaimer

Copernicus Publications remains neutral with regard to jurisdictional claims made in the text, published maps, institutional affiliations, or any other geographical representation in this paper. While Copernicus Publications makes every effort to include appropriate place names, the final responsibility lies with the authors. Views expressed in the text are those of the authors and do not necessarily reflect the views of the publisher.

Acknowledgements

We thank Dr. Tavazzani for help in obtaining compositional profiles across sample X4.

Financial support

DS was partly supported by an ETH Career Seed Award.

References

Audi, G., Bersillon, O., Blachot, J., and Wapstra, A. H.: The Nubase evaluation of nuclear and decay properties, Nuclear Physics A, 729, 3-128, https://doi.org/10.1016/j.nuclphysa.2003.11.001, 2003.

https://doi.org/10.5194/egusphere-2026-4403
Preprint. Discussion started: 7 August 2026

Bau, M., Romer, R. L., Lüders, V., and Beukes, N. J.: Pb, O, and C isotopes in silicified Mooidraai dolomite (Transvaal Supergroup, South Africa): implications for the composition of Paleoproterozoic seawater and 'dating' the increase of oxygen in the Precambrian atmosphere, Earth Planet. Sci. Lett., 174, 43-57, https://doi.org/10.1016/S0012-821X(99)00261-7, 1999.

Bowring, J. F., McLean, N. M., and Bowring, S. A.: Engineering cyber infrastructure for U-Pb geochronology: Tripoli and U-Pb_Redux, Geochem. Geophys. Geosyst., 12, Q0AA19, https://doi.org/10.1029/2010GC003479, 2011.

Chaldekas, O., Vaks, A., Haviv, I., Gerdes, A., and Albert, R.: U-Pb speleothem geochronology reveals a major 6 Ma uplift phase along the western margin of Dead Sea Transform, Geol. Soc. Am. Bull., 134, 1571-1584, https://doi.org/10.1130/B36051.1, 2021.

Chen, J. H., Edwards, R. L., and Wasserburg, G. J.: 238U, 234U and 232Th in seawater, Earth Planet. Sci. Lett., 80, 241-251, https://doi.org/10.1016/0012-821X(86)90108-1, 1986.

Chen, T., Robinson, L. F., Beasley, M. P., Claxton, L. M., Andersen, M. B., Gregoire, L. J., Wadham, J., Fornari, D. J., and Harpp, K. S.: Ocean mixing and ice-sheet control of seawater 234U/238U during the last deglaciation, Science, 354, 626-629, https://doi.org/10.1126/science.aag1015, 2016.

Cheng, H., Edwards, R. L., Hoff, J., Gallup, C. D., Richards, D. A., and Asmerom, Y.: The half-lives of uranium-234 and thorium-230, Chem. Geol., 169, 17-33, https://doi.org/10.1016/S0009-2541(99)00157-6, 2000.

Cheng, H., Edwards, R. L., Shen, C. C., Polyak, V. J., Asmerom, Y., Woodhead, J., Hellstrom, J., Wang, Y. J., Kong, X. G., Spötl, C., Wang, X. F., and Alexander, E. C.: Improvements in 230Th dating, 230Th and 234U half-life values, and U–Th isotopic measurements by multi-collector inductively coupled plasma mass spectrometry, Earth Planet. Sci. Lett., 371, 82-91, https://doi.org/10.1016/j.epsl.2013.04.006, 2013.

Chutcharavan, P. M., Dutton, A., and Ellwood, M. J.: Seawater 234U/238U recorded by modern and fossil corals, Geochim. Cosmochim. Acta, 224, 1-17, https://doi.org/10.1016/j.gca.2017.12.017, 2018.

Condon, D. J., Schoene, B., McLean, N. M., Bowring, S. A., and Parrish, R. R.: Metrology and traceability of U–Pb isotope dilution geochronology (EARTHTIME Tracer Calibration Part I), Geochim. Cosmochim. Acta, 164, 464-480, https://doi.org/10.1016/j.gca.2015.05.026, 2015.

De Bievre, P., Lauer, K. F., Le Duigon, Y., Moret, H., Muschenborn, G., Spaepen, J., Spernol, A., Vaninbroukx, R., and Verdingh, V.: The half-life of 234-U, in: Proc. Int. Conf. Chemical Nucl. Data, Measurements and Applications, Canterbury, England, edited by: Hurrell, M. L., Inst. Civil Engineers, London, 221-225, 1971.

Dirks, P. H. G. M., Kibii, J. M., Kuhn, B. F., Steininger, C., Churchill, S. E., Kramers, J. D., Pickering, R., Farber, D. L., Mériaux, A.-S., Herries, A. I. R., King, G. C. P., and Berger, L. R.: Geological setting and age of Australopithecus sediba from southern Africa, Science, 328, 205-208, https://doi.org/10.1126/science.1184950, 2010.

Drost, K., Chew, D., Petrus, J. A., Scholze, F., Woodhead, J. D., Schneider, J. W., and Harper, D. A.: An image mapping approach to U-Pb LA-ICP-MS carbonate dating and applications to direct dating of carbonate sedimentation, Geochem. Geophys. Geosyst., 19, 4631-4648, https://doi.org/10.1029/2018GC007850, 2018.

https://doi.org/10.5194/egusphere-2026-4403
Preprint. Discussion started: 7 August 2026

Engel, J., Woodhead, J., Hellstrom, J., Maas, R., Drysdale, R., and Ford, D.: Corrections for initial isotopic disequilibrium in the speleothem U-Pb dating method, Quat. Geochron., 54, 101009, https://doi.org/10.1016/j.quageo.2019.101009, 2019.

Engel, J., Woodhead, J., Hellstrom, J., White, S., White, N., and Green, H.: Using speleothems to constrain late Cenozoic uplift rates in karst terranes, Geology, 48, 755-760, https://doi.org/10.1130/g47466.1, 2020.

Gerstenberger, H. and Haase, G.: A highly effective emitter substance for mass spectrometric Pb isotope ratio determinations, Chem. Geol., 136, 309-312, https://doi.org/10.1016/S0009-2541(96)00033-2, 1997.

Gilbert, S. E. and Glorie, S.: Removal of Hg interferences for common Pb correction when dating apatite and titanite by LA-ICP-MS/MS, J. Anal. At. Spectrom., 35, 1472-1481, https://doi.org/10.1039/D0JA00224K, 2020.

Guillong, M., Wotzlaw, J. F., Looser, N., and Laurent, O.: Evaluating the reliability of U–Pb laser ablation inductively coupled plasma mass spectrometry (LA-ICP-MS) carbonate geochronology: matrix issues and a potential calcite validation reference material, Geochronology, 2, 155-167, https://doi.org/10.5194/gchron-2-155-2020, 2020.

Guillong, M., Samankassou, E., Müller, I. A., Szymanowski, D., Looser, N., Tavazzani, L., Merino-Tomé, O., Bahamonde, J. R., Buret, Y., and Ovtcharova, M.: Technical note: RA138 calcite U–Pb LA-ICP-MS primary reference material, Geochronology, 6, 465-474, https://doi.org/10.5194/gchron-6-465-2024, 2024.

Hiess, J., Condon, D. J., McLean, N., and Noble, S. R.: 238U/235U systematics in terrestrial uranium-bearing minerals, Science, 335, 1610-1614, https://doi.org/10.1126/science.1215507, 2012.

Hirata, T. and Nesbitt, R. W.: U-Pb isotope geochronology of zircon: evaluation of the laser probe-inductively coupled plasma mass spectrometry technique, Geochim. Cosmochim. Acta, 59, 2491-2500, https://doi.org/10.1016/0016-7037(95)00144-1, 1995.

Hoareau, G., Claverie, F., Pecheyran, C., Barbotin, G., Perk, M., Beaudoin, N. E., Lacroix, B., and Rasbury, E. T.: The virtual-spot approach: a simple method for image U–Pb carbonate geochronology by high-repetition-rate LA-ICP-MS, Geochronology, 7, 387-407, https://doi.org/10.5194/gchron-7-387-2025, 2025.

Hoareau, G., Claverie, F., Pecheyran, C., Paroissin, C., Grignard, P. A., Motte, G., Chailan, O., and Girard, J. P.: Direct U–Pb dating of carbonates from micron-scale femtosecond laser ablation inductively coupled plasma mass spectrometry images using robust regression, Geochronology, 3, 67-87, https://doi.org/10.5194/gchron-3-67-2021, 2021.

Holden, N. E.: Total and spontaneous fission half-lives for uranium, plutonium, americium and curium nuclides, Pure Appl. Chem., 61, 1483-1504, https://doi.org/10.1351/pac198961081483, 1989.

Hopley, P. J., Reade, H., Parrish, R., De Kock, M., and Adams, J. W.: Speleothem evidence for C3 dominated vegetation during the Late Miocene (Messinian) of South Africa, Review of Palaeobotany and Palynology, 264, 75-89, https://doi.org/10.1016/j.revpalbo.2019.02.006, 2019.

Hu, H.-M., Shen, C.-C., Cheng, H., Woodhead, J. D., Edwards, R. L., Zhao, J.-x., Huang, C.-Y., Lu, P.-Y., Chien, W.-Y., Wang, J., Jia, X., Yokoyama, Y., Cai, Y., and Zachariáš, J.: Sub-epsilon natural 234U/238U measurements refine the 234U half-life and U-Th geochronology, Sci. Adv., 11, eadu8117, https://doi.org/10.1126/sciadv.adu8117, 2025.

https://doi.org/10.5194/egusphere-2026-4403
Preprint. Discussion started: 7 August 2026

Jaffey, A. H., Flynn, K. F., Glendenin, L. E., Bentley, W. C., and Essling, A. M.: Precision measurement of half-lives and specific activities of 235U and 238U, Phys. Rev. C, 4, 1889-1906, https://doi.org/10.1103/PhysRevC.4.1889, 1971.

Jochum, K. P., Nohl, U., Herwig, K., Lammel, E., Stoll, B., and Hofmann, A. W.: GeoReM: a new geochemical database for reference materials and isotopic standards, Geostand. Geoanal. Res., 29, 333-338, https://doi.org/10.1111/j.1751-908X.2005.tb00904.x, 2005.

Kaufman, A. and Broecker, W.: Comparison of Th230 and C14 ages for carbonate materials from lakes Lahontan and Bonneville, Journal of Geophysical Research (1896-1977), 70, 4039-4054, https://doi.org/10.1029/JZ070i016p04039, 1965.

Kronfeld, J., Vogel, J. C., and Talma, A. S.: A new explanation for extreme 234U/238U disequilibria in a dolomitic aquifer, Earth Planet. Sci. Lett., 123, 81-93, https://doi.org/10.1016/0012-821X(94)90259-3, 1994.

Lounsbury, M. and Durham, R. W.: The alpha half life of 234-U, in: Chemical Nuclear Data Measurements and Applications, Emerald Publishing Limited, 215-219, https://doi.org/10.1680/cndmaa.44555.0032, 1971.

Ludwig, K. R., Simmons, K. R., Szabo, B. J., Winograd, I. J., Landwehr, J. M., Riggs, A. C., and Hoffman, R. J.: Mass-spectrometric 230Th-234U-238U dating of the Devils Hole calcite vein, Science, 258, 284-287, https://doi.org/10.1126/science.258.5080.284, 1992.

Mason, A. J., Henderson, G. M., and Vaks, A.: An acetic acid-based extraction protocol for the recovery of U, Th and Pb from calcium carbonates for U-(Th)-Pb geochronology, Geostand. Geoanal. Res., 37, 261-275, https://doi.org/10.1111/j.1751-908X.2013.00219.x, 2013.

Mason, A. J., Vaks, A., Breitenbach, S. F. M., Hooker, J. N., and Henderson, G. M.: A simplified isotope dilution approach for the U–Pb dating of speleogenic and other low-232Th carbonates by multi-collector ICP-MS, Geochronology, 4, 33-54, https://doi.org/10.5194/gchron-4-33-2022, 2022.

McLean, N. M., Condon, D. J., Schoene, B., and Bowring, S. A.: Evaluating uncertainties in the calibration of isotopic reference materials and multi-element isotopic tracers (EARTHTIME Tracer Calibration Part II), Geochim. Cosmochim. Acta, 164, 481-501, https://doi.org/10.1016/j.gca.2015.02.040, 2015.

Nuriel, P., Wotzlaw, J. F., Ovtcharova, M., Vaks, A., Stremtan, C., Šala, M., Roberts, N. M. W., and Kylander-Clark, A. R. C.: The use of ASH-15 flowstone as a matrix-matched reference material for laser-ablation U − Pb geochronology of calcite, Geochronology, 3, 35-47, https://doi.org/10.5194/gchron-3-35-2021, 2021.

Pagel, M., Bonifacie, M., Schneider, D. A., Gautheron, C., Brigaud, B., Calmels, D., Cros, A., Saint-Bezar, B., Landrein, P., and Sutcliffe, C.: Improving paleohydrological and diagenetic reconstructions in calcite veins and breccia of a sedimentary basin by combining Δ47 temperature, δ18Owater and U-Pb age, Chem. Geol., 481, 1-17, https://doi.org/10.1016/j.chemgeo.2017.12.026, 2018.

Parrish, R. R., Parrish, C. M., and Lasalle, S.: Vein calcite dating reveals Pyrenean orogen as cause of Paleogene deformation in southern England, J. Geol. Soc., 175, 425-442, https://doi.org/10.1144/jgs2017-107, 2018.

Paton, C., Hellstrom, J., Paul, B., Woodhead, J., and Hergt, J.: Iolite: Freeware for the visualisation and processing of mass spectrometric data, J. Anal. At. Spectrom., 26, 2508-2518, https://doi.org/10.1039/c1ja10172b, 2011.

https://doi.org/10.5194/egusphere-2026-4403
Preprint. Discussion started: 7 August 2026

Paton, C., Woodhead, J. D., Hellstrom, J. C., Hergt, J. M., Greig, A., and Maas, R.: Improved laser ablation U-Pb zircon geochronology through robust downhole fractionation correction, Geochem. Geophys. Geosyst., 11, https://doi.org/10.1029/2009GC002618, 2010.

Pickering, R., Kramers, J. D., Partridge, T., Kodolanyi, J., and Pettke, T.: U–Pb dating of calcite–aragonite layers in speleothems from hominin sites in South Africa by MC-ICP-MS, Quat. Geochron., 5, 544-558, https://doi.org/10.1016/j.quageo.2009.12.004, 2010.

Pickering, R., Herries, A. I. R., Woodhead, J. D., Hellstrom, J. C., Green, H. E., Paul, B., Ritzman, T., Strait, D. S., Schoville, B. J., and Hancox, P. J.: U–Pb-dated flowstones restrict South African early hominin record to dry climate phases, Nature, 565, 226-229, https://doi.org/10.1038/s41586-018-0711-0, 2019.

Pollard, T., Woodhead, J., Hellstrom, J., Engel, J., Powell, R., and Drysdale, R.: DQPB: software for calculating disequilibrium U–Pb ages, Geochronology, 5, 181-196, https://doi.org/10.5194/gchron-5-181-2023, 2023.

Pollard, T. J., Woodhead, J. D., Drysdale, R. N., Edwards, R. L., Li, X., Wainwright, A. N., Pythoud, M., Cheng, H., Hellstrom, J. C., Isola, I., Regattieri, E., Zanchetta, G., and Parmenter, D. S.: Radiometric dating of Middle Pleistocene carbonates: assessing consistency and performance of the U–Th and U–Pb dating methods, Geochronology, 7, 335-355, https://doi.org/10.5194/gchron-7-335-2025, 2025.

Porcelli, D. and Swarzenski, P. W.: The behavior of U-and Th-series nuclides in groundwater, Rev. Mineral. Geochem., 52, 317-361, https://doi.org/10.2113/0520317, 2003.

Rasbury, E. T. and Cole, J. M.: Directly dating geologic events: U-Pb dating of carbonates, Rev. Geophys., 47, https://doi.org/10.1029/2007RG000246, 2009.

Rasbury, E. T., Present, T. M., Northrup, P., Tappero, R. V., Lanzirotti, A., Cole, J. M., Wooton, K. M., and Hatton, K.: Tools for uranium characterization in carbonate samples: case studies of natural U–Pb geochronology reference materials, Geochronology, 3, 103-122, https://doi.org/10.5194/gchron-3-103-2021, 2021.

Richards, D. A., Bottrell, S. H., Cliff, R. A., Ströhle, K., and Rowe, P. J.: U-Pb dating of a speleothem of Quaternary age, Geochim. Cosmochim. Acta, 62, 3683-3688, https://doi.org/10.1016/S0016-7037(98)00256-7, 1998.

Roberts, N. M. W., Rasbury, E. T., Parrish, R. R., Smith, C. J., Horstwood, M. S. A., and Condon, D. J.: A calcite reference material for LA-ICP-MS U-Pb geochronology, Geochem. Geophys. Geosyst., 18, 2807-2814, https://doi.org/10.1002/2016GC006784, 2017.

Roberts, N. M. W., Drost, K., Horstwood, M. S. A., Condon, D. J., Chew, D., Drake, H., Milodowski, A. E., McLean, N. M., Smye, A. J., Walker, R. J., Haslam, R., Hodson, K., Imber, J., Beaudoin, N., and Lee, J. K.: Laser ablation inductively coupled plasma mass spectrometry (LA-ICP-MS) U–Pb carbonate geochronology: strategies, progress, and limitations, Geochronology, 2, 33-61, https://doi.org/10.5194/gchron-2-33-2020, 2020.

Schmitz, M. D. and Schoene, B.: Derivation of isotope ratios, errors, and error correlations for U-Pb geochronology using 205Pb-235U-(233U)-spiked isotope dilution thermal ionization mass spectrometric data, Geochem. Geophys. Geosyst., 8, Q08006, https://doi.org/10.1029/2006gc001492, 2007.

Steiger, R. H. and Jäger, E.: Subcommission on geochronology: Convention on the use of decay constants in geo- and cosmochronology, Earth Planet. Sci. Lett., 36, 359-362, https://doi.org/10.1016/0012-821X(77)90060-7, 1977.

Stirling, C. H., Andersen, M. B., Potter, E.-K., and Halliday, A. N.: Low-temperature isotopic fractionation of uranium, Earth Planet. Sci. Lett., 264, 208-225, https://doi.org/10.1016/j.epsl.2007.09.019, 2007.

Szymanowski, D., Wotzlaw, J. F., Ovtcharova, M., Schoene, B., Schaltegger, U., Schmitz, M. D., Ickert, R. B., Chelle-Michou, C., Chamberlain, K. R., Crowley, J. L., Davies, J. H. F. L., Eddy, M. P., Gaynor, S. P., Käßner, A., Mohr, M. T., Paul, A. N., Ramezani, J., Tapster, S., Tichomirowa, M., von Quadt, A., and Wall, C. J.: Interlaboratory reproducibility of ID-TIMS U–Pb geochronology evaluated with a pre-spiked natural zircon solution, Geochronology, 7, 409-425, https://doi.org/10.5194/gchron-7-409-2025, 2025.

Vaks, A., Bar-Matthews, M., Matthews, A., Ayalon, A., and Frumkin, A.: Middle-Late Quaternary paleoclimate of northern margins of the Saharan-Arabian Desert: reconstruction from speleothems of Negev Desert, Israel, Quat. Sci. Rev., 29, 2647-2662, https://doi.org/10.1016/j.quascirev.2010.06.014, 2010.

Vaks, A., Mason, A. J., Breitenbach, S. F. M., Kononov, A. M., Osinzev, A. V., Rosensaft, M., Borshevsky, A., Gutareva, O. S., and Henderson, G. M.: Palaeoclimate evidence of vulnerable permafrost during times of low sea ice, Nature, 577, 221-225, https://doi.org/10.1038/s41586-019-1880-1, 2020.

Vaks, A., Mason, A., Breitenbach, S. F. M., Giesche, A., Osinzev, A., Adrian, I., Kononov, A., Umbo, S., Lechleitner, F. A., Rosensaft, M., and Henderson, G. M.: Arctic speleothems reveal nearly permafrost-free Northern Hemisphere in the late Miocene, Nat. Commun., 16, 5483, https://doi.org/10.1038/s41467-025-60381-5, 2025.

Varga, Z., Nicholl, A., Wallenius, M., and Mayer, K.: Remeasurement of 234U Half-Life, Anal. Chem., 88, 2763-2769, https://10.1021/acs.analchem.5b04370, 2016.

Vermeesch, P.: Unifying the U–Pb and Th–Pb methods: joint isochron regression and common Pb correction, Geochronology, 2, 119-131, https://doi.org/10.5194/gchron-2-119-2020, 2020.

Vermeesch, P.: Too good to be true: Underdispersion in geochronology, EGUsphere, 2026, 1-26, https://doi.org/10.5194/egusphere-2026-2783, 2026.

Vermeesch, P., McLean, N., Vaks, A., Golan, T., Breitenbach, S. F. M., and Parrish, R.: Carbonate 206Pb/238U problems and potential 207Pb/235U fixes, Geochronology, 7, 459-473, https://doi.org/10.5194/gchron-7-459-2025, 2025.

von Quadt, A., Wotzlaw, J. F., Buret, Y., Large, S. J. E., Peytcheva, I., and Trinquier, A.: High-precision zircon U/Pb geochronology by ID-TIMS using new 1013 ohm resistors, J. Anal. At. Spectrom., 31, 658-665, https://doi.org/10.1039/c5ja00457h, 2016.

Walker, J., Cliff, R. A., and Latham, A. G.: U-Pb isotopic age of the StW 573 hominid from Sterkfontein, South Africa, Science, 314, 1592-1594, https://doi.org/10.1126/science.1132916, 2006.

Wendt, I. and Carl, C.: U/Pb dating of discordant 0.1 Ma old secondary U minerals, Earth Planet. Sci. Lett., 73, 278-284, https://doi.org/10.1016/0012-821X(85)90076-7, 1985.

https://doi.org/10.5194/egusphere-2026-4403
Preprint. Discussion started: 7 August 2026

White, W. M., Albarède, F., and Télouk, P.: High-precision analysis of Pb isotope ratios by multi-collector ICP-MS, Chem. Geol., 167, 257-270, https://doi.org/10.1016/S0009-2541(99)00182-5, 2000.

Woodhead, J., Hellstrom, J., Pickering, R., Drysdale, R., Paul, B., and Bajo, P.: U and Pb variability in older speleothems and strategies for their chronology, Quat. Geochron., 14, 105-113, https://doi.org/10.1016/j.quageo.2012.02.028, 2012.

Woodhead, J., Hellstrom, J., Maas, R., Drysdale, R., Zanchetta, G., Devine, P., and Taylor, E.: U–Pb geochronology of speleothems by MC-ICPMS, Quat. Geochron., 1, 208-221, https://doi.org/10.1016/j.quageo.2006.08.002, 2006.

Wotzlaw, J. F., Buret, Y., Large, S. J. E., Szymanowski, D., and von Quadt, A.: ID-TIMS U-Pb geochronology at the 0.1‰ level using 10 13 Ω resistors and simultaneous U and 18O/16O isotope ratio determination for accurate UO2 interference correction, J. Anal. At. Spectrom., 32, 579-586, https://doi.org/10.1039/c6ja00278a, 2017.